NRC Publications Archive
Archives des publications du CNRC

An overview of internal waves in the ocean
Zaman, Hasanat; Millan, Jim

NRC Publications Record / Notice d'Archives des publications de CNRC:
https://nrc-publications.canada.ca/eng/view/object/?id=a6d5f17e-d89c-4c00-aad3-516b13692cb7
https://publications-cnrc.canada.ca/fra/voir/objet/?id=a6d5f17e-d89c-4c00-aad3-516b13692cb7

Questions? Contact the NRC Publications Archive team at
PublicationsArchive-ArchivesPublications@nrc-cnrc.gc.ca. If you wish to email the authors directly, please see the first page of the publication for their contact information.

Vous avez des questions? Nous pouvons vous aider. Pour communiquer directement avec un auteur, consultez la première page de la revue dans laquelle son article a été publié afin de trouver ses coordonnées. Si vous n'arrivez pas à les repérer, communiquez avec nous à PublicationsArchive-ArchivesPublications@nrc-cnrc.gc.ca.

National Research Council Canada   Conseil national de recherches Canada

Canada

DOCUMENTATION PAGE

REPORT NUMBER	NRC REPORT NUMBER	DATE		
TR-2012-03		March 2012		
REPORT SECURITY CLASSIFICATION		**DISTRIBUTION**		
Unclassified		Unlimited		
TITLE An overview of **Internal waves in the ocean**				
AUTHOR (S) Hasanat Zaman and Jim Millan				
CORPORATE AUTHOR (S)/PERFORMING AGENCY (S) Institute for Ocean Technology, National Research Council, St. John's, NL				
PUBLICATION				
SPONSORING AGENCY(S) Defence R & D Canada				
IOT PROJECT NUMBER 2505-16		**NRC FILE NUMBER**		
KEY WORDS Internal waves for temparature and density variation, barotropic internal waves, loading of internal waves		**PAGES** i, 22	**FIGS.** 15	**TABLES**

SUMMARY

An overview of the ocean internal waves is documented in this report. Internal waves of different wave heights from centimetres to hundreds of metres are found in the oceans. Similarly, wavelengths vary from centimetres to hundreds of meters to tens of kilometres and periods from seconds to several hours. The generation mechanisms of the internal waves are numerous, among them internal waves due to temperature or density or salinity variation along water depth is very common. Interaction between the barotropic tide and the bottom ridges or steep bottom slope or sills or bottom seated mountains can generate large amplitude internal waves. Internal waves can be generated due to the motion of surface or under water vehicles.

ADDRESS   National Research Council
Institute for Ocean Technology
Arctic Avenue, P. O. Box 12093
St. John's, NL   A1B 3T5
Tel.: (709) 772-5185, Fax: (709) 772-2462

An overview of

Internal waves in the ocean

TR-2012-03

Hasanat Zaman and Jim Millan

March 2012

TABLE OF CONTENTS

ABSTRACT

An overview of the ocean internal waves is documented in this report. Internal waves of different wave heights from centimetres to hundreds of metres are found in the oceans. Similarly, wavelengths vary from centimetres to hundreds of meters to tens of kilometres and periods from seconds to several hours. The generation mechanisms of the internal waves are numerous, among them internal waves due to temperature or density or salinity variation along water depth is very common. Interaction between the barotropic tide and the bottom ridges or steep bottom slope or sills or bottom seated mountains can generate large amplitude internal waves. Internal waves can be generated due to the motion of surface or under water vehicles.

1.0 INTRODUCTION

Internal waves are waves in the interior of the ocean. In general internal waves are generated along the interface between two fluids of different densities or salinities. Large internal waves can also be generated when barotropic tides collide with bottom ridges or bottom seated mountains of the ocean. Internal waves transport mass, momentum and energy.

Fig. 1 Surface manifestation of internal waves in North Channel of the St. Lawrence Estuary : (http://myweb.dal.ca/kelley/SLEIWEX/results.php)

Internal waves increase stresses to submarines, offshore platforms and ships. The turbulence around submarines can be increased when the internal waves break due to the presence or by the motion of the submarines. This information might be useful in the detection of submarines in the ocean.
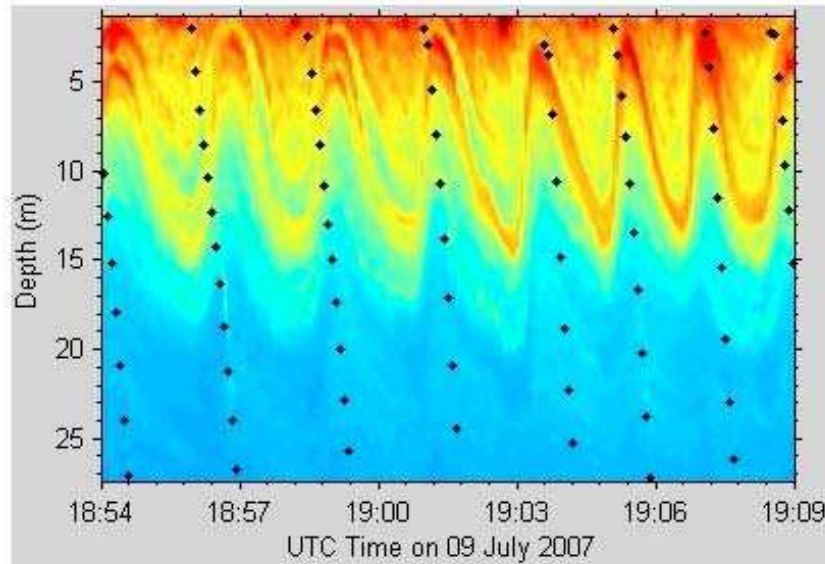
NRC·CNRC

Fig. 2 Typical internal waves in the St. Lawrence Estuary due to density stratified depth
(http://myweb.dal.ca/kelley/SLEIWEX/results.php)

Internal waves behave similarly to the waves on the surface of a body of water, but consist of the movement of regions within the water that have relatively different densities because of variations in temperature or composition due to dissolved salt. In the ocean, internal waves with large wave heights and wavelengths are usually generated when tides cause water to move over submerged mountains or ridges on the ocean floor.

Internal waves in the ocean typically have wavelengths from hundreds of meters to tens of kilometres and periods from tens of minutes to several hours. Their amplitude often exceeds 200 m.

Associated with internal waves are orbital motions of the water particles as described in Fig. 3 (the dashed circular lines). The radius of the circular motion of the water particles is largest at the pycnocline or thermocline (*see* definitions on page-3) depth and decreases downwards as well as upwards from this depth. To first order, the internal waves do not give rise to an elevation of the sea surface as the usual surface waves do, but they do give rise to a variable horizontal surface current. The current velocity at the sea surface varies in magnitude and direction giving rise to convergent and divergent flow regimes at the sea surface as mentioned in Fig. 3. The variable surface current interacts with the capillary surface waves and change the sea surface roughness (Hughes, 1978, Alpers, 1985). Due to this interaction the oceanic internal waves become visible on radar images of the sea surface and, in some cases, also on images acquired in the visible ultraviolet or infrared wavelength band (Apel et al., 1975).

Due to the hydrodynamic interaction of the variable surface currents with the surface waves, the amplitude of the Bragg waves is increased in convergent flow regions and is decreased in divergent flow regions. As a consequence, the radar signatures of oceanic internal waves consist of alternating bright and dark bands on a uniform background. Fig. 5 describes this phenomenon.

divergent   convergent   flow regime

rough   smooth   rough   smooth   sea surface
U(x)

thermocline

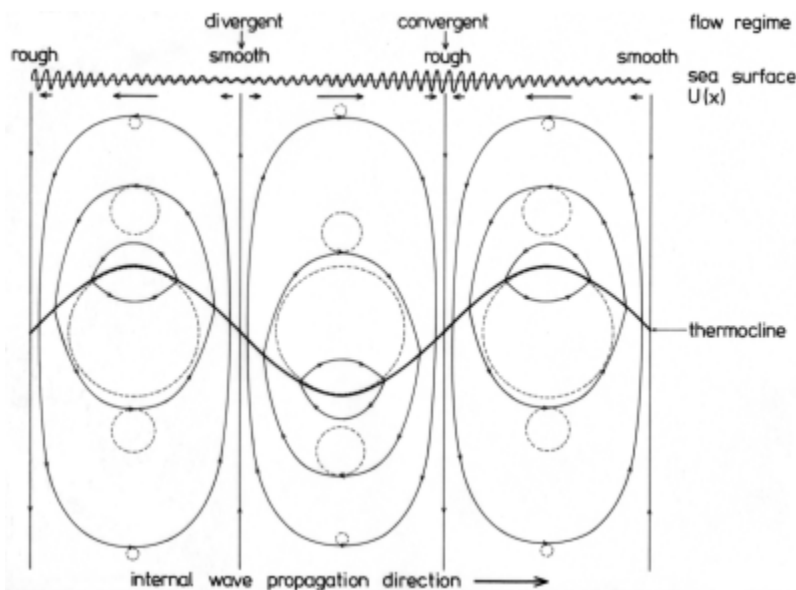internal wave propagation direction ——→

Fig. 3 Schematic plot of processes associated with the passage of a linear oceanic internal wave. Deformation of the thermocline (heavy solid line), orbital motions of the water particles (dashed lines), streamlines of the velocity field (light solid lines), surface current velocity vectors (arrows in the upper part of the image), and variation of the amplitude of the Bragg waves (wavy line at the top). [Alpers, 1985]
[http://earth.esa.int/ers/instruments/sar/applications/ERS-SARtropical/oceanic/intwaves/intro/index.html]

1.1 Some definitions:

Pycnocline : The interface between two fluids of different densities.
Thermocline : When the density difference is due to the temperature.
Halocline : The interface between two fluids of different salinity.
Interface : An unstable thin layer between the two fluids.

2.0 RADAR OBSERVATIONS OF INTERNAL WAVES

Internal waves are among the most easily recognized of the oceanographic phenomena observed in remote sensing imagery. Internal waves have long been a major concern in oceanography since they are omnipresent and can transport energy in the ocean. The characteristic signatures of alternating bands of light and dark quasi-linear strips have been noted in photographs of the sea surface, in multi-spectral radiometer images, and in real and synthetic aperture radar images. SARs became the most important remote sensors for internal wave detection. With high resolution, large spatial coverage, all-day and all weather capability, synthetic aperture radar (SAR) is a major sensor for internal wave observation. SAR is also sensitive to minor changes of ocean surface roughness produced by internal waves. Since 1970s, many images of internal waves have been captured by space-borne or air-borne SAR of different wave bands and polarizations.

These images provide abundant data to investigate internal waves in the oceans. The signatures of internal waves in SAR images are important for the identification and inversion of internal waves. Generally, internal waves can be identified as adjacent bright and dark stripes on a uniform background in SAR images shown in Fig. 4. Alpers (1988), Liu et al (1998) and Zheng et al (2001) discussed this issue elaborately in their works.

In reality, there are different types of radar signatures of short-period internal wave trains that can be very difficult to interpret. Those images suggest specific information about the characteristics of the internal waveforms that correctly interpret, provide unique measurements not only about the internal waves but also the interior ocean and the sea surface micro-layer. The fact that internal waves, especially internal solitary waves are among the most coherent and reproducible phenomena in the sea, barotropic astronomical tides perhaps excepted, makes them ideal tracers for studying characteristics of the interior ocean such as stratification (thermocline depth) as well as micro-layer parameters such as contamination by surface films.
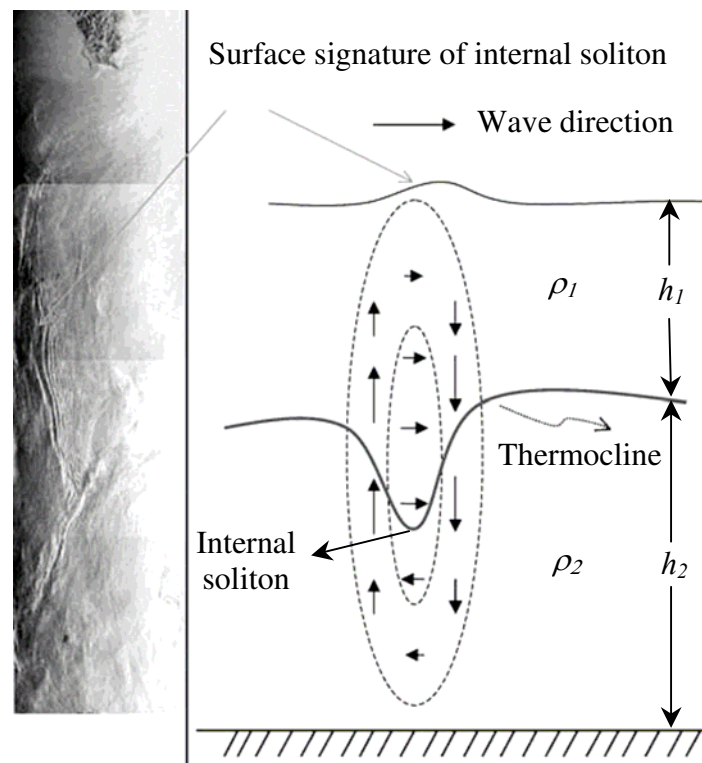

Fig. 4 An internal soliton in a two-layer fluid of finite depth is a wave of depression when $h_1 < h_2$. Sketch of internal soliton propagating on the thermocline in the coastal ocean, and structure of streamlines causing surface streak contrast with a vertical view of SAR images. A strip of 4 frames of ERS-1 SAR images (100×400 km) collected south of Taiwan in Luzon Strait on June 16, 1995, shows huge internal soliton packet located near 120°E, and 20.5°N (Hsu, et al, 2000). The solitons on the surface are produced by the convergence of water above the wave troughs in the mixed layer (Osborne and Burch, 1980).

Internal waves follow the tides and the seasons, since tidal currents are one ingredient in the recipe for producing most observed internal waves, others being stratification and variable bathymetry that perturbs the density structure.

But there exist also other radar signatures of internal waves: Sometimes they consist only of bright lines or only of dark bands. When the wind speed is below threshold for Bragg wave generation, only bright bands are encountered and when surface slicks are present, only dark lines are seen (da Silva et al., 1998). However, radar imaging theories capable of explaining these exceptional radar signatures of internal waves is not available yet.

3.0 INTERNAL WAVE CATEGORIES

3.1 Internal waves due to stratified flow

Internal waves exist when the water body consists of layers of different densities. The difference in water density is mostly due to a difference in water temperature or due to a difference in salinity. The density structure of the ocean can be approximated by two layers.
Like the well-known ocean surface waves, which are waves at the interface of two media of different density, i.e., of water and air, the internal waves are waves at the interface between two water layers of different densities. In both cases the restoring force is gravity, which is the reason why both waves sometimes are called gravity waves. These waves are generated when the interface is disturbed. In the case of surface waves, this disturbance can be caused by a stone thrown into the water or by wind blowing over the water surface.
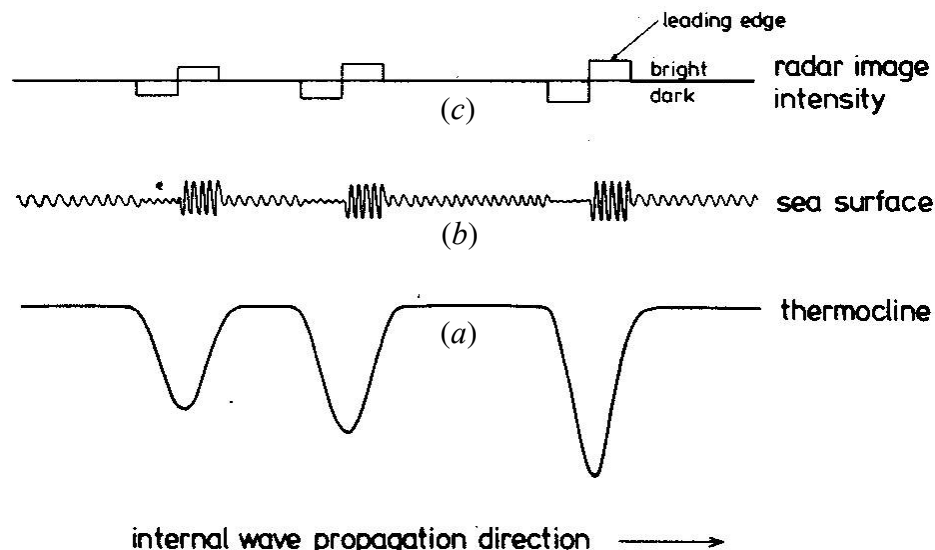

Fig. 5 (a) Shape of the thermocline, (b) sea surface roughness modulation and (c) SAR image intensity associated with an internal solitary wave packet consisting of solitons of depression of decreasing amplitude. [Alpers, 1985]

Theoretically, these highly nonlinear waves are often expressed in terms of internal solitons. Thus a wave packet contains several solitons. Since soliton theory was developed by Korteweg and De Vries (1895), hundreds of papers have been published dealing with this subject. Soliton theories applicable to the description of the generation and propagation of internal solitary waves predict that, if the depth of the upper water layer is much smaller than the depth of the lower layer, then the internal solitary wave must be a "wave of depression". This means that this soliton is associated with a depression of the pycnocline as depicted schematically in Fig. 5 and as measured in the ocean (see Fig. 6) at strait of Messina on October 25, 1995. The leading edge of a soliton of depression is always associated with a convergent surface current region and the trailing edge with a divergent region. At the front of the soliton the amplitude of the Bragg waves is increased, while at the rear it is decreased. According to Bragg scattering theory, the normalized radar cross section is proportional to the amplitude squared of the Bragg wave (Valenzuela, 1978).
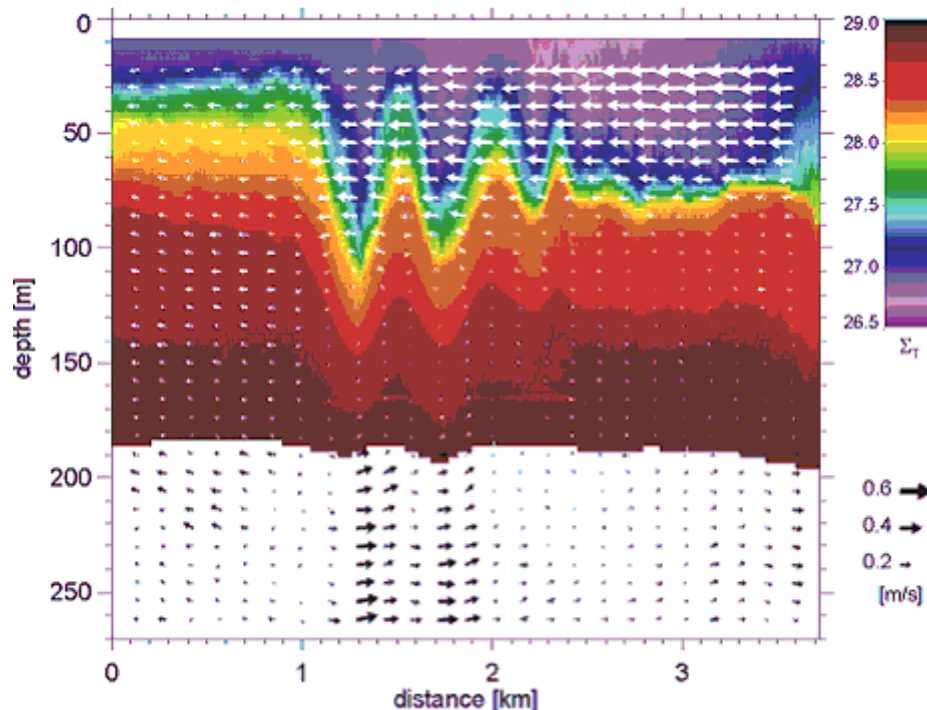

Fig. 6 Density and current distributions measured in the Mediterranean Sea north of the Strait of Messina during the passage of a northward propagating packet of internal solitary waves. The density distribution was measured by a CTD (conductivity temperature, depth) chain (Sellschopp, 1997) and the current distribution by an acoustic Doppler current profiler from the research ship "Alliance" (Figures by P. Brandt and A. Rubino, Institute of Oceanography, University of Hamburg).
[http://earth.esa.int/ers/instruments/sar/applications/ERS-SARtropical/oceanic/intwaves/intro/index.html]

This is the reason why on SAR images the front section of a soliton of depression is bright, and the rear section dark (Defant, 1961, Alpers, 1985). As mentioned before, the

radar signatures of internal solitary waves may deviate from this scheme when surface slicks are present or the wind speed is low.

3.2   Internal waves due to tides

In the case of internal waves, this disturbance is usually caused by tidal flow pushing the layered water body over shallow underwater obstacles, e. g., over shallow sills or shallow ridges (Maxworthy, 1975, Helferich et al., 1984, Lamb, 1994). Akylas et. al. (2011) described from field observations data that large-amplitude internal solitary waves in deep water, far far away from the continental shelf, can alternatively be generated.
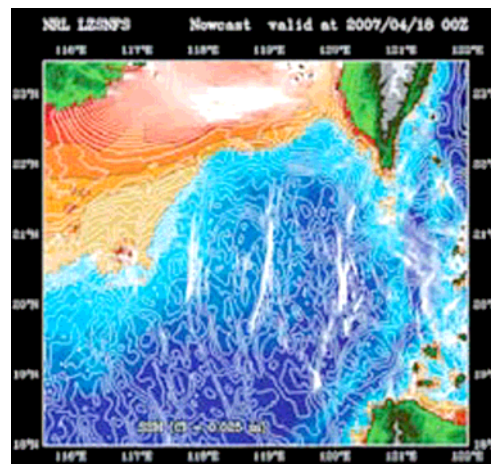

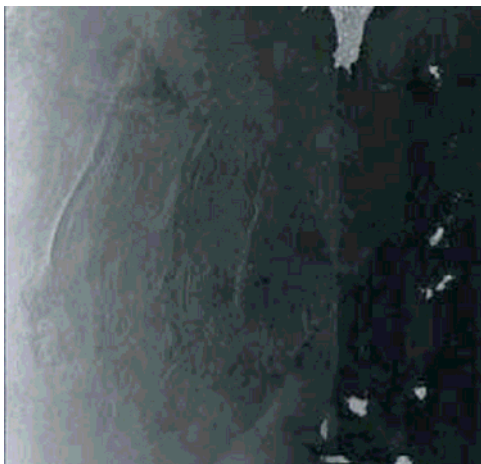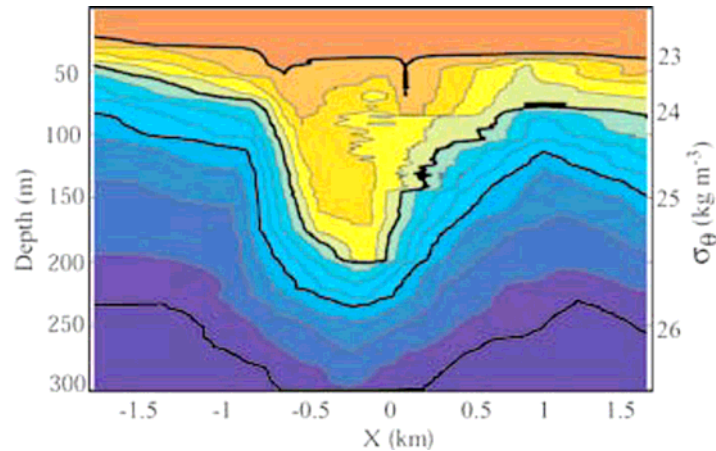Fig 7. Internal waves generated by barotropic tide (Ko et al, 2008) in the South China Sea have amplitudes over 200 m (top) and extend over 200 km (bottom left and right).

The mechanism is tidal flow over steep topography forces a propagating beam of internal tidal wave energy which impacts the thermocline at a considerable distance from the forcing site and produces internal solitary waves there. Boegman, L. and Aghsaee, P.

(2011) have investigated the breaking of shoaling internal solitary waves upon uniformly sloping bottom topography both numerically and experimentally. They observed over steep slope all three distinct breaking mechanisms: surging, plunging and collapsing breakers, related with reflection, convective instability and flow separation. Internal tides can generate large amplitude solitary internal waves. The U.S. Office of Naval Research (ONR) finances studies of ocean internal waves using an integrated and interdisciplinary team to answer the questions about the generation, fate, and transformation of internal tides and internal waves in the ocean. They worked on the South China Sea project and on the shelf of New Jersey and addressed the processes governing the transformation from internal tide to non-linear internal solitary waves (Paluszkiewicz, 2011). The tidally generated internal waves are usually highly nonlinear and occur often in wave packets. The distance between the waves in a wave packet and also the amplitude decreases from the front to the back. In recent years very large amplitude of internal waves are observed in the South China Sea (Helfrich and Melville, 2006). Ko et al (2008) have shown that underwater ridges can transform the barotropic tides into internal tides.

Internal tides undergo steepness change and their other characteristics change and convert into internal bores that later modify into large amplitude internal solitary waves. These internal waves are estimated to be over 200 meters in amplitude and their crests extend over more than 200 km. These evanescent large-amplitude internal waves can drive water up or down a couple of hundred meters in minutes and significantly interrupt the safe operation of submerged vehicles, such as less powerful unmanned undersea vessels (UUV).

The interaction of quasi-steady currents with the bottom topography is found to produce an internal wave drag and associated momentum flux of approximately 0.5 dyn/cm^2, which is comparable to the average wind stress on the ocean surface (Bell Jr, 1975). The interaction of the barotropic tide with the bottom topography is found to result in a flux of energy of order 1 erg/cm^{2}s into the internal tide. Considering both the rate of input of energy into the internal tides and the rate of loss from them it is perceived that internal tides are probably not a significant sink for energy extracted from the surface tide. This mechanism appears to be capable of supplying a significant portion of the observed internal wave energy in the ocean. The internal tide is probably dissipated by inherently nonlinear phenomena: spectral transport by weak interactions and, in the upper oceans, strong interactions manifested by localized instabilities resulting in isolated patches of turbulence. Internal tides can generate large amplitude solitary internal waves. In the absence of the tide, internal waves can be generated by the frontal instability of the Kuroshio-current or by Kuroshio-current and bottom topography interaction, but this energy is much weaker than the internal energy produced by the tides. The semidiurnal tide is more effective in producing the large-amplitude internal waves than the diurnal tide. A tabulation of worldwide observations suggests that internal semidiurnal tides contain 10–50% of the energy of the surface tide (Wunsch, 1975).

3.3 Internal waves by moving structure

Internal waves can be generated by a moving submerged body that can be a submarine or any other under water vehicles. Chang et al (2008) described the generation of the internal waves by submarine using RANS equation. Fig. 8 shows the computational

domain. They showed the distribution of the internal wave heights due to the motion of a submarine in a two layer fluids. They assumed that the fresh water depth was 45m and salt water depth was 100m. They put the submarine in the fresh water layer in such a way that the distance between the interface of the two fluids and the longitudinal axis of the submarine was 15m. Figs. 9 to 12 show the distribution of the internal wave heights with varying Froude number ($F_r^2 = u^2/g(h_1 + h_2)$). In their results they described that with the increase of the Froude number the wave length increased. They argued that there were transverse wave and divergent wave in the interface simultaneously when the Froude number of moving submarine was less than the critical Froude number of the internal wave pattern, but there would only be divergent wave in the interface when the Froude number of moving submarine was larger than the critical Froude number of internal wave pattern.
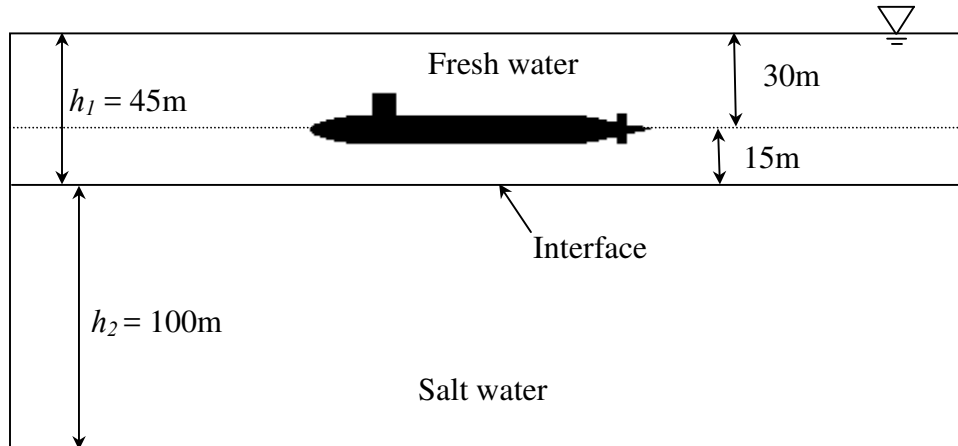

Fig. 8 Definition sketch of the problem [Chang et al, 20]
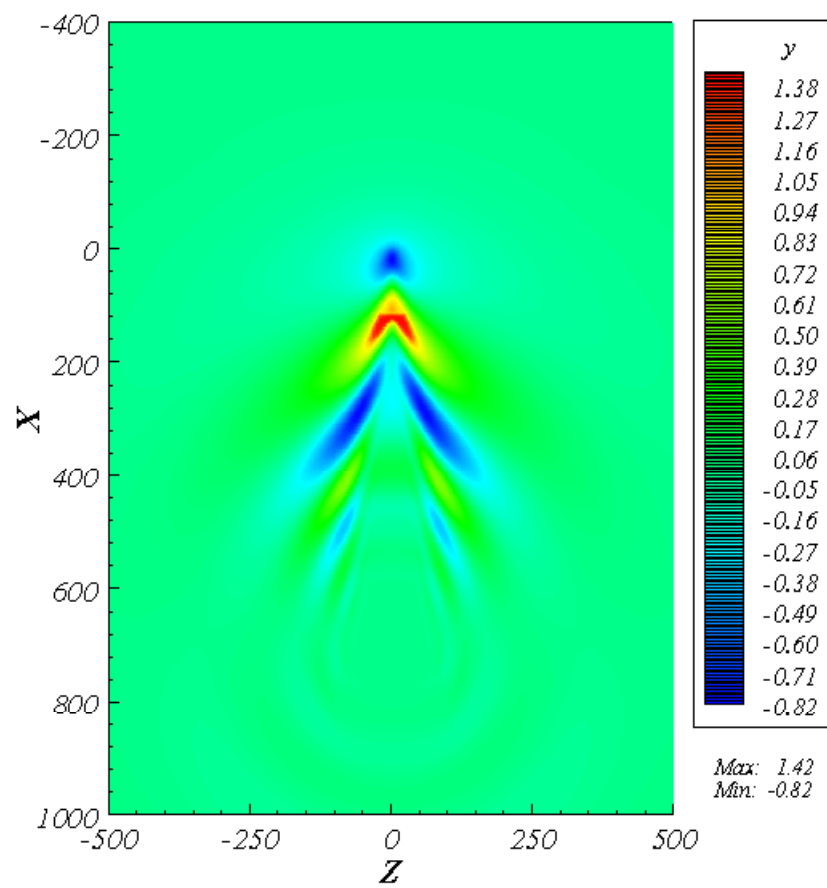
Fig. 9 Internal wave height for Froude number, Fr=0.068 [Chang et al, 2008]
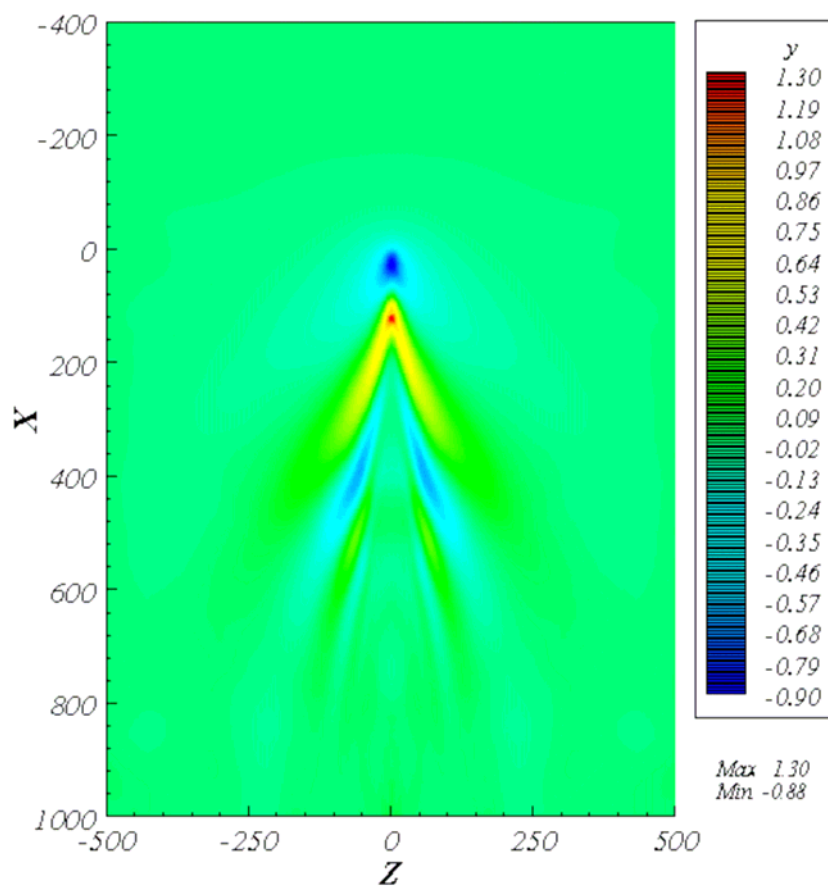
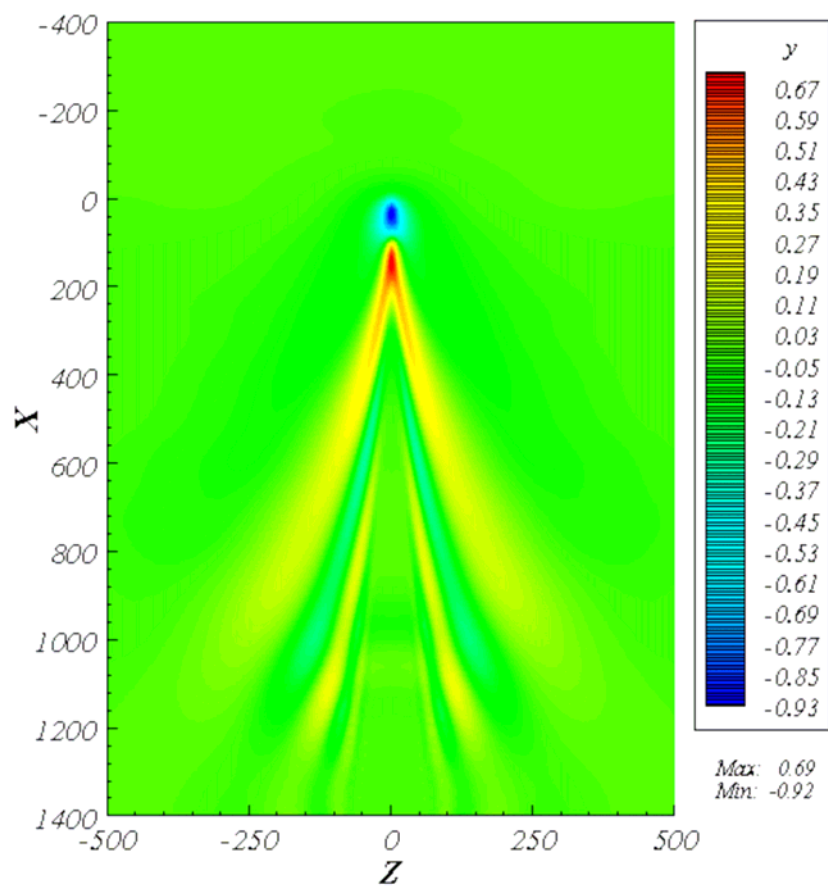Fig. 10 Internal wave height for Froude number, Fr=0.095 [Chang et al, 2008]

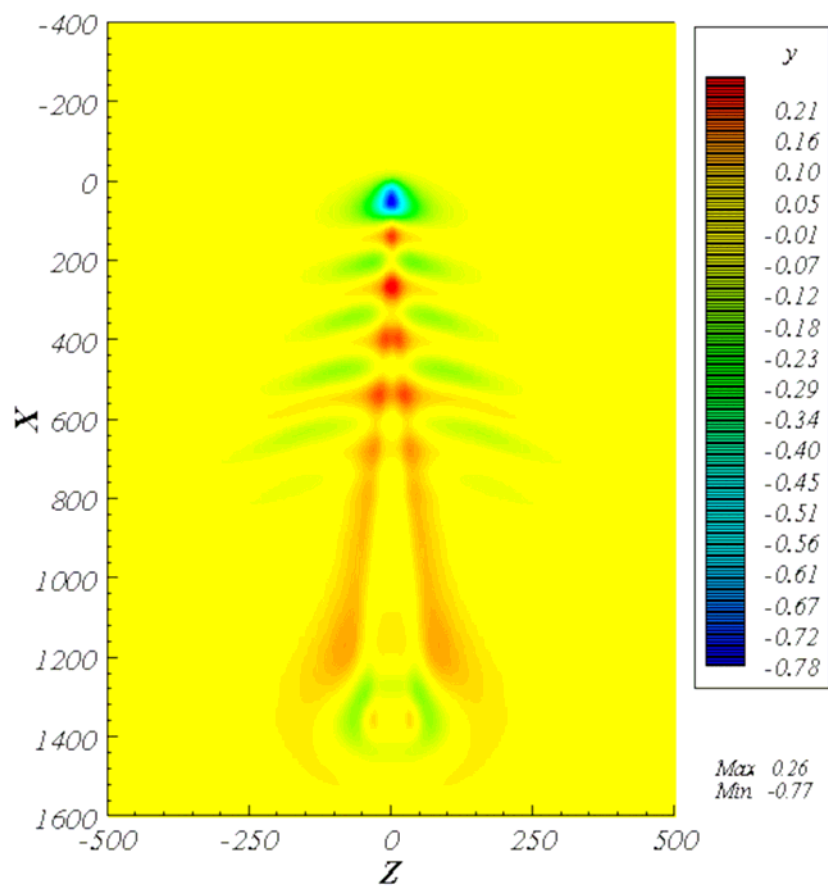Fig. 11 Internal wave height for Froude number, Fr=0.164 [Chang et al, 2008]

Fig. 12 Internal wave height for Froude number, Fr=0.312 [Chang et al, 2008]

4.0 DEAD WATER PHENOMENON

Another interesting phenomena caused by internal gravity waves is dead-water. When a boat is travelling over water that strongly resembles a two layer fluid, a thin light layer of fresh water at the top and a thick dense layer of salt or cold water below, the boat is unexpectedly slowed down by a mysterious force. The force is due to the ship generating a wake of waves at the interface of the two layers. The energy that the ship exerts to propel itself forward is translated into the generation of the internal waves.
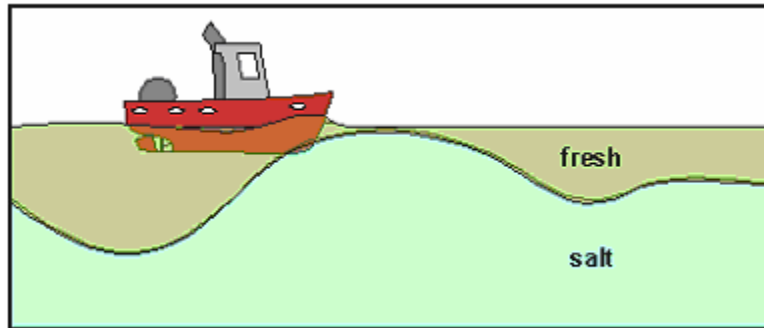
Fig. 13 Dead water by internal waves on the free surface due to slow moving ship

Dead water initiates when a ship enters a fjord zone where fresh lighter water lies on top of the heavier salt water. Watch videos here: www.youtube.com/watch?v=PCOL8kUtufg and www.nioz.nl/nioz_nl/281c18dbf72fc51c599b4f49dddc1143.php. Slow ships then unintentionally start an internal wave, making it larger as the ship is pushing it forward. This instant wave produces higher resistance to the ship to move forward and it appears as if the ship has stopped or dead in the water.
(http://www.seafriends.org.nz/oceano/waves2.htm)

Fig. 14 Dead water by internal waves along the layer of fluids of different densities

Dead water phenomenon might be extrapolated for underwater vehicles that entering an interface of fluids of different densities or salinities. In dead water a boat may experience strong resistance due to high drug to forward motion in apparently calm conditions. The e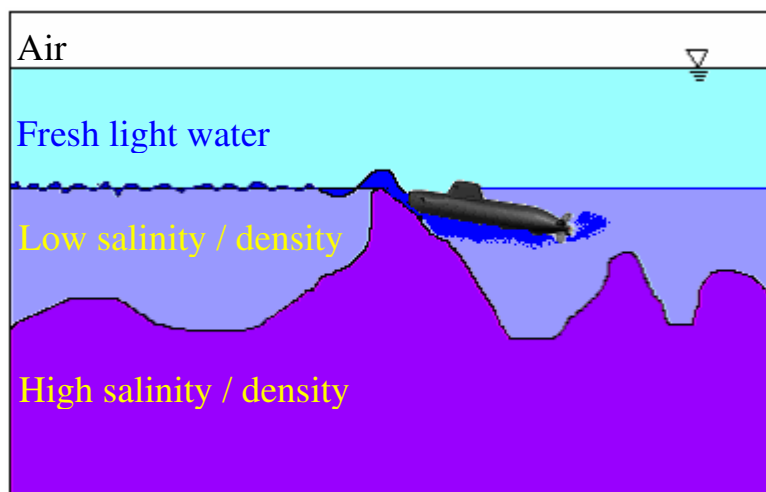ffect of dead water is much more on the slow moving vehicles or an underwater vehicle, such as a submarine that is moving slowly to or out of the parking dock. In the worst case the vehicle can not move forward at all.

5.0 THEORY OF INTERNAL WAVES

5.1 Gravity waves in a two-layer fluid

Like surface waves, gravity is the restoring force for internal waves. To model internal waves mathematically, we first consider a two layer fluid, that is, a fluid which has two layers each with different density, the denser layer is located on the bottom.
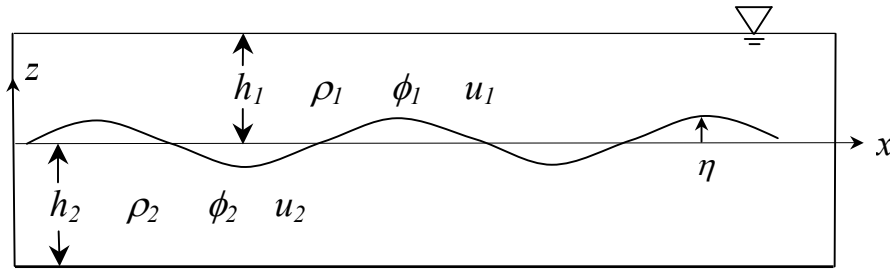
Fig. 15 Schematic view of internal waves along the interface of a two-layered fluid

Fig. 15 describes internal waves in two-layered fluids of different density.

If we assume that the fluid is incompressible and irrotational then the potential function for each layer solves Laplace's equation.

$$\nabla^2 \phi_1 = 0 \tag{1}$$

$$\nabla^2 \phi_2 = 0 \tag{2}$$

where ϕ_1 and ϕ_2 respectively, are the velocity potentials at the upper and the lower layers of the fluids.

At the interface between the two fluids, the vertical velocity components in both layers of fluids must be the same and also the pressure at the interface should be identical. This gives the following two boundary conditions at the interface which we refer to as kinematic and dynamic boundary conditions, respectively:

$$\frac{\partial \eta}{\partial t} = \frac{\partial \phi_1}{\partial z} = \frac{\partial \phi_2}{\partial z} = w \qquad at \quad z = 0 \tag{3}$$

$$\rho_1 \frac{\partial \phi_1}{\partial t} + \rho_1 g \eta = \rho_2 \frac{\partial \phi_2}{\partial t} + \rho_2 g \eta \qquad at \quad z = 0 \tag{4}$$

where, η is the undulation along the boundary of the fluids, ρ_1 and ρ_2 are densities, w is the vertical velocity component and g is the gravitational acceleration.

Since we are interested in simple harmonic motion, we specify the interface motion as

$$\eta = a \cos(kx - \sigma t) \tag{5}$$

where a is the wave amplitude, k and σ are the interfacial wave number and frequency, respectively.

The velocity potential for the upper layer of the fluid can be defined as (Buick and Greated, 1998)

$$\phi_1 = \frac{ia\sigma \cosh k(z - h_1)}{k \sinh kh_1} \cos(kx - \sigma t) \tag{6}$$

Similarly the velocity potential for the bottom layer would be defined as

$$\phi_2 = \frac{ia\sigma \cosh k(z + h_2)}{k \sinh kh_2} \cos(kx - \sigma t) \tag{7}$$

The dispersion relation or the relation between wave number k and wave frequency σ can be obtained when Eqs. 5 to 7 are inserted into Eq. 4 as

$$\sigma^2 = gk(\rho_2 - \rho_1) \frac{\tanh kh_1 \tanh kh_2}{\rho_1 \tanh kh_2 + \rho_2 \tanh kh_1} \tag{8}$$

The expressions for the internal fluid velocities can be obtained from the derivatives of the velocity potentials Eqs. 6 and 7.

$$u_1 = \frac{\partial \phi_1}{\partial x} = -\frac{ia\sigma \cosh k(z - h_1)}{\sinh kh_1} \sin(kx - \sigma t) \tag{9}$$

$$u_2 = \frac{\partial \phi_2}{\partial x} = -\frac{ia\sigma \cosh k(z + h_2)}{\sinh kh_2} \sin(kx - \sigma t) \tag{10}$$

$$w = \frac{\partial \phi_1}{\partial x} = \frac{\partial \phi_2}{\partial x} = -\frac{ia\sigma \sinh k(z + h_2)}{\sinh kh_2} \cos(kx - \sigma t) \tag{11}$$

Now Eqs. 5 to 8 provide a complete solution for the internal waves along the boundaries of the two fluids.

5.2 Internal solitary waves

In the ocean internal solitary waves are often generated by the propagation of internal tides. An internal soliton is produced when bottom ridges or sills interact with internal tides. Interaction of internal tide beam with the thermocline or pycnocline undulation can generate large amplitude internal waves. The theory of internal solitary waves was initiated by Keulegan (1953) and Long (1956) who investigated two-fluid systems with fixed upper boundaries. A theory is derived by Benjamin (1965) that included both solitary and periodic cnoidal waves that can propagate in the stratified fluid without changing its form. Internal solitary waves can be described by the KdV equation, the KP equation and the BO equation (Gear and Grimshaw, 1983; Michallet and Barthelemy, 1998).
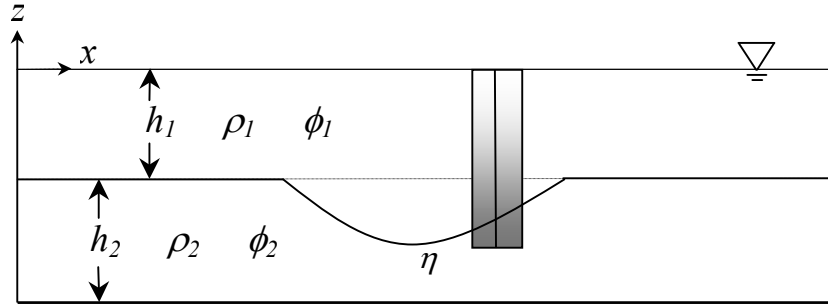
Fig. 16 Definition sketch of the domain

The propagation of nonlinear internal waves in the x horizontal direction can be described by the KdV equation (Osborne and Burch, 1980, Song et al, 2011) as

$$\frac{\partial \eta}{\partial t} + (C + \alpha\eta)\frac{\partial \eta}{\partial x} + \beta\frac{\partial^{3}\eta}{\partial x^{3}} = 0 \tag{12}$$

where η is the interface undulation of the internal waves; C, α and β are the phase speed, the coefficient of the first-order nonlinear term and the dispersion term, respectively. The expressions for C, α and β can be given as

$$C = \left[\frac{2g(\rho_{2} - \rho_{1})h_{1}h_{2}}{(\rho_{1} + \rho_{2})(h_{1} + h_{2})}\right]^{\frac{1}{2}} \tag{13}$$

$$\alpha = \frac{3C(h_{1} - h_{2})}{2h_{1}h_{2}} \tag{14}$$

$$\beta = \frac{C h_1 h_2}{6} \qquad (15)$$

where ρ_1 and ρ_2 are the densities of the upper and the lower fluid, respectively; h_1 and h_2 the depths of the layers, respectively.

A solution of Eq. (12) can be found in the following form:

$$\eta = -\eta_s \sec h^2 \left(\frac{x - C_s t}{l} \right) \qquad (16)$$

where η_s is the amplitude of the internal soliton, C_s is the phase speed and l is the scale length.

Expressions for C_s and l are as follows

$$C_s = C \left[1 - \frac{\eta_s (h_1 - h_2)}{2 h_1 h_2} \right] \qquad (17)$$

$$l = 2 h_1 h_2 / \sqrt{3 \eta_s (h_2 - h_1)} \qquad (18)$$

Based on the internal solitary wave theory the x horizontal water particle velocity (Osborne and Burch, 1980) can be expressed as

$$u_1(x,t) = \frac{C \eta_s}{h_1} \sec h^2 \left(\frac{x - C_s t}{l} \right) \qquad (19)$$

$$u_2(x,t) = -\frac{C \eta_s}{h_2} \sec h^2 \left(\frac{x - C_s t}{l} \right) \qquad (20)$$

Substituting the horizontal velocity components (Eqs. 19-20) in the following continuity equation

$$\frac{\partial u}{\partial x} + \frac{\partial w}{\partial z} = 0 \qquad (21)$$

the vertical velocity components can be obtained in the upper and lower layers as

$$w_1 = \frac{2 C \eta_s z}{h_1 l} \sec h^2 \left(\frac{x - C_s t}{l} \right) \tanh \left(\frac{x - C_s t}{l} \right) \qquad (22)$$

$$w_2 = \frac{2 C \eta_s (h_1 + h_2 + z)}{h_2 l} \sec h^2 \left(\frac{x - C_s t}{l} \right) \tanh \left(\frac{x - C_s t}{l} \right) \qquad (23)$$

The pressure at depth z can be obtained by the Bernoulli equation

$$p_1 = -\rho_1\left(gz + \frac{\partial\phi_1}{\partial t} + \frac{1}{2}(u_1^2 + w_1^2)\right) \tag{24}$$

$$p_2 = -\rho_2\left(\frac{\rho_1}{\rho_2}g(-h_1) + g(z + h_1) + \frac{\partial\phi_2}{\partial t} + \frac{1}{2}(u_2^2 + w_2^2)\right) \tag{25}$$

where g is the acceleration due to gravity; u_1 and u_2 and w_1 and w_2 are the horizontal and the vertical velocities of water particles in both layers; ϕ_1 and ϕ_2 are the velocity potentials in both layers.

Like surface solitons the internal soliton can also propagate long distances in the ocean without any distortion in its form, so the time derivative and the special derivative have the following relationship

$$\frac{\partial\phi_j}{\partial t} = -C_s\frac{\partial\phi_j}{\partial x} = -C_s u_j \qquad j = 1, \ 2 \tag{26}$$

The dynamic pressures in layer 1 (p_{d1}) and in layer 2 (p_{d2}) due to the motion of the internal soliton can be expressed as follows

$$p_{d1} = -\rho_1\left(\frac{\partial\phi_1}{\partial t} + \frac{1}{2}(u_1^2 + w_1^2)\right) = -\rho_1\left(-C_p u_1 + \frac{1}{2}(u_1^2 + w_1^2)\right) \tag{27}$$

$$p_{d2} = -\rho_2\left(\frac{\partial\phi_2}{\partial t} + \frac{1}{2}(u_2^2 + w_2^2)\right) = -\rho_2\left(-C_p u_2 + \frac{1}{2}(u_2^2 + w_2^2)\right) \tag{28}$$

6.0 LOADING ON STRUCTURE DUE TO INTERNAL WAVES

Morison's equation is very efficient in force computation on any object when the diameter (D) of the object is 5 times greater than the local wave length (L), *i.e.* when $5D > L$. For large objects diffraction theory is appropriate to compute loads. Morison's Equation for the inline force per unit length of circular cylinder can be written in the following forms

$$F_1 = \frac{1}{2}\rho_1 C_{D1} D u_1 |u_1| + \rho_1 C_{M1} A \frac{\partial u_1}{\partial t} + \rho_1 A \frac{\partial u_1}{\partial t}$$

$$F_2 = \frac{1}{2}\rho_2 C_{D2} D u_2 |u_2| + \rho_2 C_{M2} A \frac{\partial u_2}{\partial t} + \rho_2 A \frac{\partial u_2}{\partial t}$$

where F_1 and F_2 are the forces per unit length of circular cylinder in layers 1 and 2, respectively. D is the diameter, A is the cross sectional area of the cylinder, C_{D1} and C_{D2} and, C_{M1} and C_{M2} are the drag and inertia coefficients.

It should be noted that if the structure is large enough compared to the wave length, a diffraction wave theory must be used for a better prediction of the load.

7.0 CONCLUSIONS

Internal waves can be found everywhere in the ocean. The wave heights of such internal waves can be centimetres to several hundred metres. The reason for the occurrence of these internal waves is due to differences in the water temperature and density over the water depth. The interaction of internal tides with the bottom ridges, sills or bottom seated mountains can generate large amplitude internal waves. A beam of internal tide can interact with thermocline-, halocline- or pycnocline-type internal waves and can generate soliton-type internal waves. Internal waves can be hazardous for surface vessels to propel forward. The motion of slow moving underwater vehicles can be affected by internal waves. Large amplitude internal waves can exert considerable loads on the underwater vehicles.

REFERENCES

Akylas, T. R., Grimshaw, R. H. J., Tabaei, A. and Clarke, S.R. (2011): Theoretical model for local generation of solitary waves by reflecting wave beams in the ocean thermocline, Conference in Les Houches (France), Organized by Thierry Dauxois (ENS Lyon) and Thomas Peacock (MIT).

Alpers, W. (1985): Theory of radar imaging of internal waves, *Nature*, **314**, 245-247.

Apel, J.R., Byrne, H.M., Proni, J.R. & Charnell, R.L. (1975): Observation of oceanic internal and surface waves from the Earth Resources Technology Satellite, *J. Geophys. Res.*, **80**, 865-881.

Bell Jr, T. H. (1975): Topographically generated internal waves in the open ocean, *J. Geophys. Res.*, **80(3)**, 320-327.

Benjamin, T. B. (1965): Internal waves of finite amplitude and permanent form, *J. Fluid Mech*, 25, 241-270.

Boegman, L. and Aghsaee, P. (2011): Breaking of and resuspension beneath shoaling internal solitary waves, Conference in Les Houches (France), Organized by Thierry Dauxois (ENS Lyon) and Thomas Peacock (MIT).

Buick, J. M. and Greated, C. A. (1998): Lattice Boltzmann modeling of interfacial gravity waves, Physics of fluids, American Institute of Physics, **10(6)**, 1490-1511.

Chang, Y, Zhao, F., Zhang, J., Hong F-W., Li, P. and Yun, J. (2008): Numerical simulation of internal waves excited by a submarine moving in the two-layer stratified fluid, Conference of Global Chinese Scholars on Hydrodynamics.

Chen, C.-Y., Hsu, J. R.-C., Chen, C.-W., Chen, H.-H., Kuo, C.-F., and Cheng, M.-H. (2007): Generation of internal solitary wave by gravity collapse, *J. of Marine Science and Tech*, **15**(1), pp. 1-7.

da Silva, J.C.B., Ermakov, S.A., Robinson, I.S., Jeans, D.R.G. & Kijashko, S.V. (1998): Role of surface films in ERS SAR signatures of internal waves on the shelf, 1. Short-period internal waves, *J. Geophys. Res.*, 8009-8031.

Defant, A., (1961): Physical oceanography, Pergamon, Oxford, **2**, 517-570.

Gear, J. A. and Grimshaw, R. (1983): A second-order theory for solitary waves in shallow fluids Physics of Fluids, **26 (1)**, 14–29.

Helfrich, K.R. & Melville, W.K. (1986): On long nonlinear internal waves over slope-shelf topography, *J. Fluid Mech.*, **167**, 285-308.

Helfrich, K.R. and Melville, W. K. (2006): Long nonlinear internal waves, Annual *Review of Fluid Mech.*, **38**, 395-425.

Hsu, M.-K., Liu, A.K. & Liu, C. (2000): A study of internal waves in the China Seas and Yellow Sea using SAR, *Continental Shelf Research*, **20**, 389-410.

Hughes,B.A. (1978): The effect of internal waves on surface wind waves, 2, Theoretical analysis, *J. Geophys. Res.*, **83**, 455-465.

Keulegan, G. H. (1953): Characteristics of internal solitary waves, J. Res., National Bureau of Standards, **52**, 133.

Ko, D.S., Martin, P.J., Chao, S.Y, Shaw, P.T. and Lien, R.C. (2008) : Large-Amplitude Internal Waves in the South China Sea, Report of NRL (Naval Research Laboratory) review, SW, Washington (ONR sponsored).

Korteweg, D.J. & de Vries, G. (1895): On the change of long waves advancing in a rectangular canal and a new type of long stationary waves, *Phil. Mag.*, **5**, 422.

Lamb, K.G. (1994): Numerical experiments of internal wave generation by strong tidal flow across a finite amplitude bank edge, *J. Geophys. Res.*, **99**, 843-864.

Liu, A.K., Chang, Y.S., Hsu, M. and Liang, N. K. (1998): Evolution of nonlinear internal waves in the East and South China Sea," *J. Geophys. Res.*, **103(C4)**, 7995–8008.

Long, R. R. (1956): Solitary waves in one- and two-fluid systems, Tellus, **8**, 460.

Maxworthy, T. (1979): A note on the internal solitary waves produced by tidal flow over a three-dimensional ridge, *J. Geophys. Res.*, **84**, 338-346.

Michallet, M. and Barthelemy, E. (1998): Experimental study of interfacial solitary waves, *J. of Fluid Mech*, **336**, 159–177.

Miyata, Motoyasu, URL http://iprc.soest.hawaii.edu/~miyata/IWavesPublicationList.htm

Osborne, A.R. and Burch, T.L. (1980): Internal Solitons in the Andaman Sea, *Science*, **208(4443)**, 451- 460.

Paluszkiewicz, T. (2011): An Overview of Internal Wave Research Programs at ONR, Conference in Les Houches (France), Organized by Thierry Dauxois (ENS Lyon) and Thomas Peacock (MIT).

Sellschopp, J. (1997): A towed CTD chain for high-resolution hydrography, *Deep-Sea Res.*, **44**, 147-165.

Song, Z. J., Teng, B., Gou, Y., Lu, L., Shi, Z.M., Xiao, Y. and Qu, Y. (2011): Comparisons of internal solitary wave and surface wave actions on marine structures and their responses, Applied Ocean Research, 33(2), 120–129.

Valenzuela, G.R. (1978): Theories for the interaction of electromagnetic and ocean waves, A review, *Boundary Layer Meteorol.*, **13**, 61-85.

Wunsch, C. (1975): Internal tides in the ocean, *Revues of Geophysics*, 13(1), 167-182.

Zheng, Q., Yuan, Y., Klemas, V. and Yan, X.-H. (2001): Theoretical expression for an ocean internal soliton synthetic aperture radar image and determination of the soliton signature half width," *J. Geophys. Res.*, vol. 106, no. C11, pp. 31 415–31 423.

NRC·CNRC